Physics of Plasmas

Thermal confinement bifurcation and the L- to H-mode transition in tokamaks

Cite as: Physics of Fluids B: Plasma Physics 3, 696 (1991); https://doi.org/10.1063/1.859866
Submitted: 31 July 1990 . Accepted: 24 October 1990 . Published Online: 04 June 1998

F. L. Hinton


View Online

Export Citation

ARTICLES YOU MAY BE INTERESTED IN

Influence of sheared poloidal rotation on edge turbulence
Physics of Fluids B: Plasma Physics 2, 1 (1990); https://doi.org/10.1063/1.859529

Neoclassical poloidal and toroidal rotation in tokamaks
Physics of Fluids B: Plasma Physics 3, 2050 (1991); https://doi.org/10.1063/1.859671

Effects of $E\times B$ velocity shear and magnetic shear on turbulence and transport in magnetic confinement devices
Physics of Plasmas 4, 1499 (1997); https://doi.org/10.1063/1.872367

AIP Publishing

© 1991 American Institute of Physics.

Thermal confinement bifurcation and the L- to H-mode transition in tokamaks

F. L. Hinton
General Atomics, San Diego, California 92186-9784

(Received 31 July 1990; accepted 24 October 1990)

A bifurcation in the thermal confinement of tokamaks, which resembles the L- to H-mode transition, is shown to follow from properties of edge turbulence recently derived by Biglari *et al.* [Phys. Fluids B 2, 1 (1990)], and the standard neoclassical theory of poloidal rotation. The temperature profiles develop a pedestal at the plasma edge, and the poloidal rotation near the edge is considerably increased, when the heating power exceeds a critical value. The energy confinement time is a discontinuous function of increasing heating power, but is continuous for decreasing power (power hysteresis). Critical values of density and magnetic field are found, which must be exceeded in order for the bifurcation to occur. The scaling of the power threshold with density, magnetic field, and ion mass is similar to what is found experimentally.

I. INTRODUCTION

One of the most important problems in current fusion research is to understand the H mode of improved confinement in tokamaks, discovered by the ASDEX group,[1] and subsequently confirmed and elaborated upon by many other groups on other tokamaks. The L-mode to H-mode transition is characterized by the sudden development of significantly improved particle and energy confinement near the plasma edge. This sudden change of the edge conditions suggests a bifurcation, but theoretical understanding of it has been elusive. A threshold amount of heating power is needed for the transition to H mode, although the type of heating used (neutral beam, ion cyclotron resonance, electron cyclotron resonance, or Ohmic) does not seem to matter. A theory that can predict the power threshold as a function of plasma parameters is needed to extrapolate the present experimental confinement results to ignition devices.

Recently, spectroscopic measurements of poloidal and toroidal plasma flows on the DIII-D tokamak[2] have shown that the poloidal rotation increases suddenly and significantly during the L- to H-mode transition, and remains large in the H mode. This has lead to speculation that poloidal rotation or the electric field associated with it may be playing a causal role in the transition. Although the mechanism for reducing the fluctuations and transport near the edge during the L- to H-mode transition has not been understood, it is reasonable to assume that it is related in some way to changes in poloidal rotation.

Shaing and Crume[3] have proposed that a bifurcation in the poloidal rotation is responsible for the improvement in confinement, although the connection between poloidal rotation and confinement was left somewhat vague. Their bifurcation depends upon the balance of poloidal torques having more than one solution for the poloidal rotation speed, where the curve of a (postulated) radial current-induced torque versus rotation speed crosses the curve of poloidal rotation damping, the latter being a nonlinear function of rotation speed because of approximations that lead to a resonance in the rotation damping. However, this resonance effect may not be present in tokamaks of low aspect ratio, such as the DIII-D tokamak.

In this paper, a bifurcation in the thermal confinement, which resembles the L- to H-mode transition and which involves poloidal rotation, is shown to follow from properties of edge turbulence recently derived by Biglari *et al.*[4] Only the standard neoclassical theory of poloidal rotation[5,6] is needed. Neither the resonance effect of Shaing and Crume nor the radial current that they postulated is used.

Biglari *et al.*[4] found that sheared poloidal rotation affects the decorrelation process for ambient edge turbulence and leads to a suppression of the turbulence below its ambient value. The turbulent quench mechanism was found to be insensitive to the sign of the rotation or its shear. A simple formula for the turbulent thermal conductivity that has these properties is assumed here: the turbulent thermal conductivity decreases with increasing poloidal rotation shear and is independent of its sign.

It is also assumed here that the poloidal rotation is given by the standard neoclassical expression, proportional to the ion temperature gradient, where the coefficient of proportionality is a function of the ion collisionality, and therefore of the ion temperature. Taking the poloidal rotation shear to be due primarily to the variation of this proportionality coefficient, near the plasma edge, leads to a particular nonlinear dependence of the thermal conductivity on the ion temperature gradient, and this is responsible for the bifurcation. It is assumed here that the ion and electron temperatures are equal, and that the only energy loss is by thermal conduction.

The resulting expression for the heat flux across the plasma edge, as a function of the temperature gradient, has a maximum and a minimum, which implies a jump in the edge temperature gradient as the heat flux is increased. The temperature profiles obtained with model heating profiles show a significant temperature pedestal, when the power exceeds a threshold value, similar to the experimental profiles.[1] The energy confinement times obtained when the power threshold is just barely exceeded are larger than

 0899-8213/91/030696-09$02.00 © 1991 American Institute of Physics

those for powers slightly less than the threshold, by a significant factor. Hysteresis in the confinement time versus heating power is found also, as in the experiments,[7] with different confinement times obtained with increasing and decreasing heating power, within a certain range of heating powers. The scaling of the H-mode power threshold, with plasma density, toroidal magnetic field, and ion mass, agrees in some respects with the experimental scalings.[7,8] Critical values for the density and magnetic field strength, which must be exceeded to achieve the H mode, are predicted by this model; the former has been seen experimentally.[1]

Since some of the coefficients in the ion thermal conductivity model have numerical values that are not known, no attempt is made here to compare with the experimental numbers. Only the qualitative predictions of the theory are compared with the experiment.

The paper is organized as follows. The properties of neoclassical poloidal rotation are discussed in Sec. II. In Sec. III, the suppression of edge turbulence by sheared poloidal rotation is discussed. The thermal conductivity models used in this paper are presented in Sec. IV, and the temperature and poloidal flow profiles derived from the constant coefficient model are given in Sec. V. In Sec. VI, energy confinement times for this model are given, and the hysteresis phenomenon is exhibited. A more realistic model, which is consistent with the power degradation of energy confinement in the L mode, is presented in Sec. VII, and the scaling of the H-mode power threshold with plasma parameters is discussed in Sec. VIII. A discussion of the results is given in Sec. IX, and the results are briefly summarized in Sec. X.

II. NEOCLASSICAL THEORY OF POLOIDAL ROTATION

Useful information is obtained from the lowest-order ion momentum balance and particle conservation,

$$n_i e(-\nabla\Phi + \mathbf{u}_i \times \mathbf{B}/c) = \nabla p_i, \tag{1}$$

$$\nabla\cdot(n_i\mathbf{u}_i) = 0. \tag{2}$$

The magnetic field is assumed to be described by the usual flux coordinates, such that

$$\mathbf{B} = B_\phi \hat{e}_\phi + (\hat{e}_\phi/R)\times\nabla\psi, \tag{3}$$

where ψ is the poloidal flux function. The ion density is assumed to be constant on a magnetic surface, $n_i = n_i(\psi)$, and the radial mass flow is neglected: $\mathbf{u}_i\cdot\nabla\psi \simeq 0$. Then the mass flow velocity $\mathbf{u}\equiv\mathbf{u}_i$ must have the form

$$\mathbf{u} = \omega(\psi) R \hat{e}_\phi + K_i(\psi)\mathbf{B}, \tag{4}$$

where ω is related to the radial electric field and ion pressure gradient, and K_i must be determined using kinetic theory. In the circular cross-section approximation, which will frequently be used for simplicity,

$$\omega(r) = -\frac{c}{RB_\theta}\left(\frac{\partial\Phi}{\partial r} + \frac{1}{n_i e}\frac{\partial p_i}{\partial r}\right). \tag{5}$$

The perpendicular and poloidal flows, although in nearly the same direction in tokamaks, are given by different expressions:

$$\mathbf{u}_\perp = c[(\hat{b}\times\nabla\Phi)/B] + [(c\mathbf{b}\times\nabla p_i)/n_i eB], \tag{6}$$

$$\mathbf{u}_p = K_i\mathbf{B}_p. \tag{7}$$

Actually, Eq. (6) is best understood as determining the electric field for a given perpendicular flow, which may be equal to the poloidal flow, when $u_p \ll (B_\phi/B_p)u_p$.

In standard neoclassical theory,[5] the poloidal flow is shown to be proportional to the temperature gradient, independent of the radial electric field. A temperature gradient causes a poloidal torque to appear on the ions, as a result of the dependence of ion collision frequency on ion energy. This torque drives the poloidal flow against the rotation damping due to magnetic pumping.[6] A poloidal flow driven in this way can induce a radial electric field, according to the ion momentum equation. In particular, if the temperature gradient suddenly increases with no change in the toroidal angular momentum, then the resulting perpendicular flow will induce a radial electric field.

Standard neoclassical theory[5] gives (again using the circular cross-section approximation)

$$u_\theta = -\frac{c}{eB}\mu_i\frac{\partial T_i}{\partial r}, \tag{8}$$

where the coefficient of proportionality μ_i has different limiting values (with opposite signs) in the two asymptotic regimes of collisionality. In particular, in the Pfirsch–Schlüter regime of large collisionality, its value is $\mu_i = 1.7$.

The sign agrees with the experimental rotation direction in DIII-D, for the usual direction of the toroidal magnetic field.[2] Also, it is found experimentally that the poloidal rotation direction is reversed when the direction of the toroidal magnetic field is reversed,[8] and this can be shown to also follow from neoclassical theory (see the Appendix). The direction of poloidal rotation is found to be consistent with a negative radial electric field, for either sign of toroidal magnetic field, and this is consistent with the previous equations. The poloidal rotation measurements in DIII-D are actually of the He^{++} impurity; it is assumed here that the poloidal rotation of the main ions is approximately the same. Although the experimentally measured poloidal rotation speeds are somewhat larger than predicted by neoclassical theory, the errors in the measurements are difficult to estimate, and it seems not unreasonable to assume that they do not disagree significantly with the prediction of neoclassical theory. Also, since the radial gradients are so large in the experiment, the theory may need to be improved, but the result would probably have the same form with a different numerical value for the coefficient μ_i.

The ion collisionalities that occur in the DIII-D experiment[7] are in the range of 1–5, which is not large enough for the asymptotic Pfirsch–Schlüter regime value to be ap-

propriate. The coefficient μ_i in Eq. (8) is actually a function of collisionality, which is needed in the following section.

The parallel component of the ion momentum equation and the toroidal component of the total momentum equation (neglecting small terms) are

$$m_i n_i \frac{\partial}{\partial t}\langle \mathbf{B}\cdot\mathbf{u}_i\rangle = -\langle \mathbf{B}\cdot(\nabla\cdot\mathbf{\Pi}_i)\rangle, \tag{9}$$

$$m_i n_i \frac{\partial}{\partial t}\langle \mathbf{u}_i\cdot\hat{e}_\phi R\rangle = -\langle R\hat{e}_\phi\cdot(\nabla\cdot\mathbf{\Pi}_i)\rangle + \frac{1}{c}\langle \mathbf{j}\cdot\nabla\psi\rangle. \tag{10}$$

Thus radial current affects toroidal rotation, but not parallel flow. The time derivative of parallel flow can be written in terms of the time derivatives of poloidal and toroidal flows. The steady-state poloidal flow equation contains a small term proportional to the time derivative of the toroidal rotation, which is neglected here. The steady-state parallel momentum equation,

$$\langle \mathbf{B}\cdot(\nabla\cdot\mathbf{\Pi}_i)\rangle = 0, \tag{11}$$

determines the poloidal flow, independently of any radial current.

It is shown in the Appendix that the steady-state poloidal flow for large collisionality, ν_{*i}, is given by

$$u_\theta = -\frac{c}{eB}\mu(\nu_{*i})\frac{\partial T}{\partial r}, \tag{12}$$

where the proportionality coefficient has the form

$$\mu(\nu_{*i}) \simeq \mu_0 + \mu_1/(\nu_{*i})^2, \tag{13}$$

with $\mu_0 = 1.7$ (the Pfirsch–Schlüter regime limit), and $\mu_1 < 0$.

III. SUPPRESSION OF EDGE TURBULENCE BY SHEARED POLOIDAL ROTATION

By using a general analysis, Biglari *et al.*[4] found that sheared poloidal rotation tends to suppress ambient turbulence, and therefore turbulent transport. Although they did not distinguish between the $\mathbf{E}\times\mathbf{B}$ flow and the poloidal rotation, they implied that it is, in fact, the $\mathbf{E}\times\mathbf{B}$ flow that is the more fundamental in affecting the properties of turbulence resulting from microinstabilities. This equilibrium flow, related to the radial electric field by

$$u_E = -(c/B)E_r, \tag{14}$$

is given in terms of the poloidal and toroidal flows and the pressure gradient by the lowest-order ion momentum equation:

$$u_E = u_\theta - \frac{B_\theta}{B}u_\phi - \frac{c}{eBn_i}\frac{\partial p_i}{\partial r}, \tag{15}$$

in which $B_\phi/B \simeq 1$ has been used. In the following, the r dependence of B is neglected, as well as the second derivative terms and the terms proportional to B_θ/B. The radial shear in this flow is then given by the following:

$$\frac{\partial u_E}{\partial r} = \frac{\partial u_\theta}{\partial r} + \frac{c}{eBn_i^2}\frac{\partial n_i}{\partial r}\frac{\partial p_i}{\partial r}. \tag{16}$$

In this paper, the second term will be omitted for simplicity, and no further distinction between u_E and u_θ will be made. The analysis therefore does not, strictly speaking, apply to the very edge of the plasma, where the density gradient can be larger than the temperature gradient, in some experiments.

Using Eq. (12), with $\nu_{*i} \propto n_i/T_i^2$, the poloidal rotation shear is

$$\frac{\partial u_\theta}{\partial r} = -\frac{c}{eB}\left[\mu_i'(\nu_{*i})\left(\frac{\nu_{*i}}{n}\frac{\partial n}{\partial r} - \frac{2\nu_{*i}}{T}\frac{\partial T}{\partial r}\right)\frac{\partial T}{\partial r} + \mu_i(\nu_{*i})\frac{\partial^2 T}{\partial r^2}\right]. \tag{17}$$

The second derivative term is assumed here to be negligible. For simplicity, the density gradient term that results from the density dependence of collisionality will also be ignored. The derivative of the proportionality coefficient is $\mu_i'(\nu_{*i}) = -2\mu_1(\nu_{*i})^{-3}$, and so

$$\frac{\partial u_\theta}{\partial r} = -\frac{4c\mu_1}{eB(\nu_{*i})^2 T}\left(\frac{\partial T}{\partial r}\right)^2. \tag{18}$$

Note that the coefficient of $(\partial T/\partial r)^2$ in this expression is proportional to $T^3 n^{-2}$.

IV. THERMAL CONDUCTIVITY MODELS

The thermal conductivity is assumed to be the sum of the ion neoclassical contribution[5] and a turbulent contribution that is modified by poloidal rotation shear:

$$\kappa = \kappa_n + \frac{\kappa_a}{1+\gamma_a(\partial u_\theta/\partial r)^2}. \tag{19}$$

The poloidal rotation shear is assumed to be given by the neoclassical expression, Eq. (18). Then, the thermal conductivity is a function of the temperature gradient as follows:

$$\kappa = \kappa_n + \frac{\kappa_a}{1+\lambda_a(\partial T/\partial r)^4}, \tag{20}$$

where

$$\lambda_a = \gamma_a(4c\mu_1/eBT)^2(\nu_{*i})^{-4}. \tag{21}$$

The coefficients κ_n, κ_a, and λ_a are taken to be constants in this section. A model with $\kappa_a \propto \partial T/\partial r$ is considered in Sec. VII.

The local heat flux as a function of the temperature gradient $g \equiv -\partial T/\partial r$ is

$$\mathcal{Q}(g) \equiv \kappa_n g + \kappa_a g/(1+\lambda_a g^4). \tag{22}$$

This function has a maximum and a minimum if $\kappa_a/\kappa_n > \frac{16}{9}$, which is a reasonable assumption; it is shown in Fig. 1 for $\kappa_a/\kappa_n = 4$.

Figure 1 can be interpreted as follows. At the boundary point, $r = a$, the gradient is determined by the solution of the equation

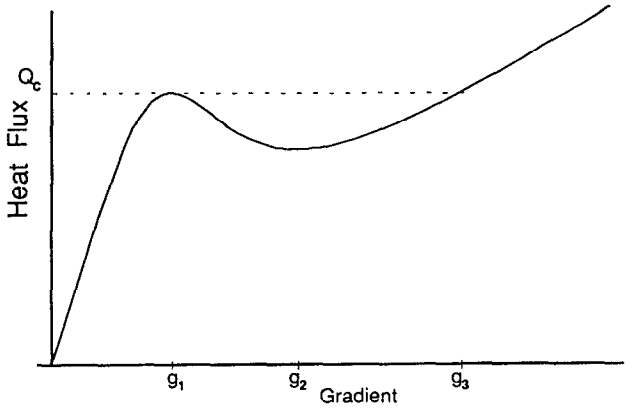

FIG. 1. Local heat flux versus temperature gradient.

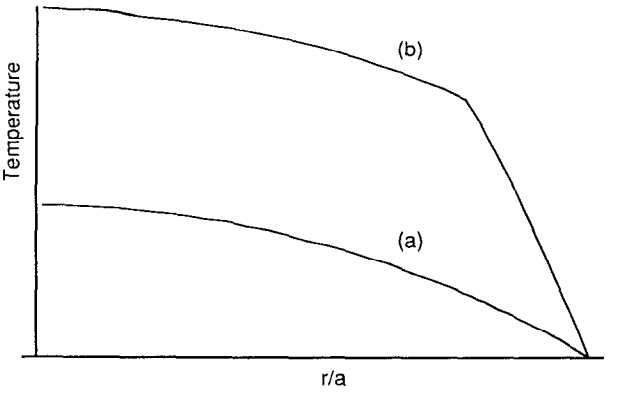

FIG. 2. Temperature profiles near the power threshold (arbitrary units): (a) $Q(a)=0.99Q_c$; (b) $Q(a)=1.01Q_c$.

$$\mathcal{Q}(g)=Q(a), \tag{23}$$

where $Q(a)$ is the heat flux across the boundary. At low power $Q(a)$, the thermal conductivity is $\kappa_n + \kappa_a$. The edge temperature gradient is small, since the poloidal rotation shear is not yet large enough to suppress the edge turbulence; this is the L mode. As $Q(a)$ is increased, the edge temperature gradient increases continuously up to g_1, but for $Q(a)$ larger than $Q_c \equiv \mathcal{Q}(g_1)$, the gradient must jump to a larger value. The poloidal rotation shear suppression of the turbulent L-mode thermal conductivity forces the solutions to have gradients larger than g_3; this is the H mode. The critical value Q_c is the power threshold for the H mode. At sufficiently high power, the turbulent thermal conductivity is completely suppressed, and the thermal conductivity has the neoclassical value κ_n.

V. TEMPERATURE AND POLOIDAL FLOW PROFILES

The equilibrium temperature profile is now determined by numerical integration of the equation

$$-\kappa\frac{dT}{dr}=Q(r), \tag{24}$$

where $Q(r)$ is the heat flux at radius r, the integral of the power deposition profile. The heating is assumed to be uniform, so the heat flux varies linearly with r:

$$Q(r)=Q(a)r/a. \tag{25}$$

Equation (24) is integrated inward, starting at $r=a$, with $T(a)=0$. It is necessary at each radius r to solve the equation

$$\mathcal{Q}(g)\equiv\kappa_n g+\kappa_a g/(1+\lambda_a g^4)=Q(r), \tag{26}$$

for the gradient $g\equiv -dT/dr$. Since all other energy loss mechanisms are ignored, the heat flux at the edge $Q(a)$ is also the total heating power.

Recall that κ_n, κ_a, and λ_a are taken to be constants. Since the numerical values of these coefficients are not known, no attempt will be made to retain physical units, and all results will therefore be expressed in "arbitrary units."

The results obtained with $\kappa_n=1$, $\kappa_a=4$, and $\lambda_a=1$ can be summarized as follows.

(a) *L mode.* If the edge heat flux $Q(a)$ is less than the power threshold Q_c, the small gradient root must be used over the entire range from $r=a$ to $r=0$. A profile like the lower curve in Fig. 2 is obtained.

(b) *H mode.* If the edge heat flux is greater than the power threshold Q_c, the integration must start on the large gradient root and stay on this branch from $r=a$ to $r=a\mathcal{Q}(g_2)/Q(a)$, where this root becomes imaginary. Then the small root must be used to continue the integration to $r=0$. The jump in slope in the temperature profile occurs at the point where the jump was made from the large root for the gradient to the small root. A profile like the upper curve in Fig. 2 is obtained. The rule used in choosing the correct branch of the solution for the gradient is that the temperature profile must be as smooth as it can be, and can have a jump in slope only when it is forced to by the disappearance of a real root. Also, since the middle root with $g_1<g<g_2$ in Fig. 1 is unstable, it is not used.

The temperature profiles shown in Fig. 2 were obtained with edge heat fluxes slightly larger and slightly smaller than the power threshold. The main distinguishing feature of the H-mode profile is the significant edge "pedestal," which occurs because of the finite interval near the edge where the gradient is between g_2 and g_3. In the L-mode profile, by contrast, the gradient is always less than g_1.

Figure 3 shows the temperature and the poloidal flow for these same two heating powers. The poloidal flow was calculated using the neoclassical expression Eq. (12), with the density and magnetic field taken to be uniform. From the analysis given in Sec. II, it is clear that, for $\nu_{*i}\gg 1$, the proportionality coefficient has the temperature dependence

$$\mu(\nu_{*i})\simeq c_0-c_1T^4. \tag{27}$$

The values $c_0=c_1=1$ were used in making Fig. 3.

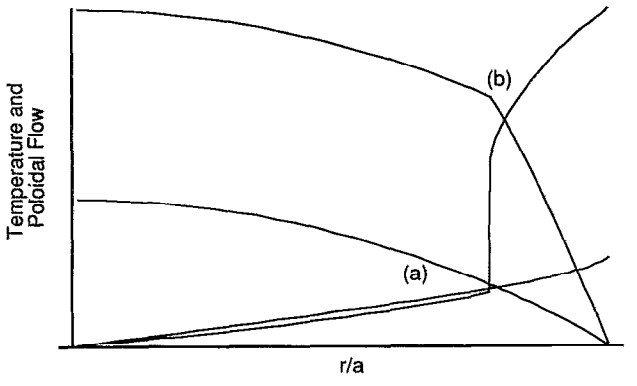

FIG. 3. Temperature and poloidal flow profiles near the power threshold (arbitrary units): (a) $Q(a) = 0.99Q_c$; (b) $Q(a) = 1.01Q_c$.

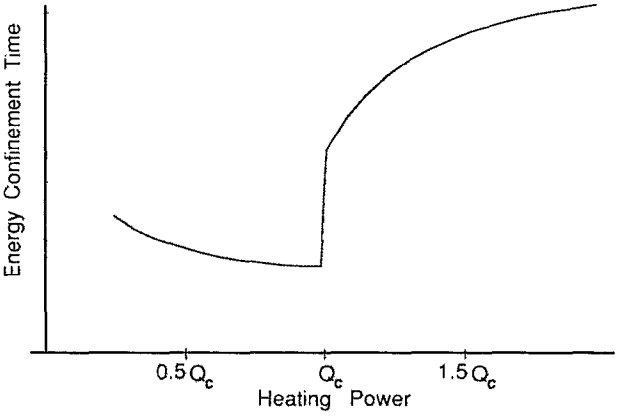

FIG. 5. Scaling of energy confinement time with heating power (arbitrary units) for the temperature-gradient-dependent model.

VI. ENERGY CONFINEMENT AND HYSTERESIS

By integrating under these curves to obtain the energy content, the global energy confinement time is obtained:

$$\tau_E \equiv \frac{\int_0^a r\,dr\,nT}{Q(a)}. \tag{28}$$

A constant factor depending on units is ignored here. By taking a constant density, $n = n_0$, for simplicity, the ratio of the confinement times, for the H- and L-mode cases with nearly the same heating power shown in Fig. 2, was found to be 3.0.

The energy confinement time is plotted versus heat flux in Fig. 4 for a range of heat fluxes. The hysteresis curve was obtained by first increasing the heating power through the critical value, and then decreasing it.

The rule used in obtaining the hysteresis curve is that the sequences of equilibria, for increasing and decreasing values of heating power, are as continuous as they can be; small changes in the amount of heating power should correspond to small changes in the profiles, whenever possible. When the heating power is increasing, the edge gradient must jump to a larger value when the power exceeds the power threshold Q_c. This causes the confinement time to be a discontinuous function of power. When the heating power is decreasing, the gradient must stay on the same branch of the solution until the power is less than the minimum in the heat flux versus gradient curve, when it is forced to jump to a lower value. The sequence of equilibria is continuous in the latter case, since the edge region of large gradient becomes very thin as the power approaches the minimum, and there is no difference in the profiles just before and just after the jump to the small gradient branch.

Hysteresis is seen experimentally:[7] once the H mode is achieved, less heating power than the power threshold is required to stay in the H mode.

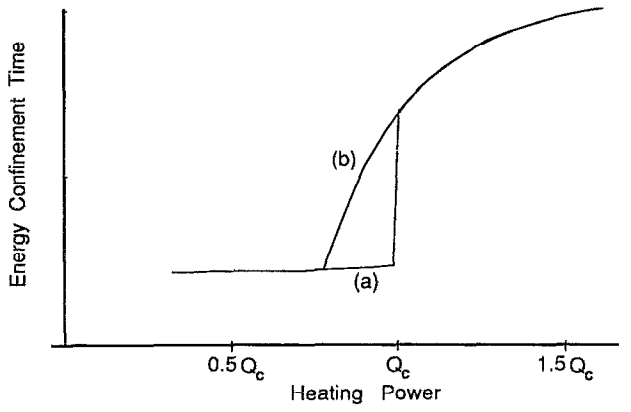

FIG. 4. Power hysteresis in the energy confinement time (arbitrary units): (a) increasing power; (b) decreasing power.

VII. A TEMPERATURE-GRADIENT-DEPENDENT MODEL

Next consider a model in which the L-mode turbulent thermal conductivity is not constant, but given by

$$\kappa_a = \kappa_{a0} g, \tag{29}$$

proportional to the temperature gradient. The confinement time for this model is shown as a function of heating power in Fig. 5. The parameters used were $\kappa_n = 1$, $\kappa_{a0} = 6$, and $\lambda_a = 1$.

(a) *L mode.* Neglecting the κ_n and λ_a terms in the thermal conductivity expression, the temperature profile and confinement time may easily be obtained analytically, with the result that the energy confinement time depends upon heating power:

$$\tau_E \propto Q(a)^{-1/2}. \tag{30}$$

There is degradation of energy confinement with heating power, similar to the experimental L-mode confinement time scaling.[9] This is also found numerically, as shown in Fig. 5.

(b) *H mode.* The confinement time increases by a factor of 2.3 when the power threshold is exceeded. In the asymptotic large power limit, the confinement time is de-

termined completely by κ_n. However, in the transitional range of powers, the coefficient κ_{a0} plays a role, as shown in Fig. 5. The confinement time approaches the H-mode value gradually as power is increased because there is still a significant portion of the plasma volume that has the small gradient characteristic of an L-mode. Degradation of confinement with power is not found, contrary to the experimental results.[8]

VIII. POWER THRESHOLD SCALING

It is important to understand the scaling of the H-mode power threshold with plasma parameters, in order to be able to extrapolate to ignition devices. In DIII-D, the power threshold is approximately linear in n and B, independent of plasma current.[7] In JET,[10] the power threshold varies roughly as $B^{1.5}$.

In order to determine the power threshold scaling predicted by this thermal confinement model, it is necessary to postulate some dependence of the parameters κ_{a0}, λ_a on plasma parameters. The temperature-gradient-dependent model of Sec. VII is used here.

The condition for turbulence suppression is given by Biglari *et al.*,[4] as

$$\frac{du_\theta}{dr} \gtrsim \frac{\Delta\omega_t}{k_y \Delta r_t}, \tag{31}$$

where $\Delta\omega_t$ is the decorrelation rate and Δr_t and k_y^{-1} are the radial and poloidal spatial correlation lengths of the ambient turbulence. Assuming drift wave turbulence,[11] $\Delta\omega_t/k_y \sim c_s\rho_s/L_n$ and $\Delta r_t \sim \rho_s$, where $c_s = (T_e/m_i)^{1/2}$, and $\rho_s = c_s/\Omega_i$, with $\Omega_i = eB/m_ic$, and L_n is the density gradient length. Thus the turbulence suppression condition is

$$\frac{du_\theta}{dr} \gtrsim \frac{c_s}{L_n}. \tag{32}$$

If resistive magnetohydrodynamic (MHD) turbulence[12] is assumed, $\Delta\omega_t \sim (L_n/R)^{1/2}(c_s/L_n)$ and $\Delta r_t \sim k_y^{-1}$, so the condition is the same as for drift wave turbulence, except for the factor $(L_n/R)^{1/2}$. This does not depend upon plasma parameters in a significantly different way, so the drift wave condition will be used.

The coefficient of the poloidal rotation shear dependence will therefore be taken to be $\gamma_a = (L_n/c_s)^2$, which depends only on temperature and ion mass. (The unknown numerical factor is set equal to 1.)

The power threshold scaling with density is found by using for the neoclassical ion thermal conductivity $\kappa_n \propto n^2$. The turbulent contribution is assumed to be similar, $\kappa_{a0} \propto n^2$, although other possibilities are discussed in Sec. IX. Also, $\lambda_a \propto n^{-4}$, which follows from $\lambda_a = \gamma_a(T^3n^{-2})^2$ and $\gamma_a \propto T^{-1}$. The result is shown in Fig. 6.

There is a critical density, below which there is no H-mode transition, because there is no maximum in the curve of heat flux versus temperature gradient below this critical density, as shown in Fig. 7. Such a critical density has been seen experimentally.[1]

Concerning the magnetic field scaling, note that the coefficient of the temperature gradient in the neoclassical poloidal rotation expression is inversely proportional to the magnetic field strength: $\mu_i(\nu_{*i}) \propto 1/B$. Hence the coefficient λ_a in the temperature gradient dependence in the thermal conductivity depends on the magnetic field as $\lambda_a \propto 1/B^2$. It is assumed that κ_n and κ_{a0} do not depend upon B at constant plasma current.

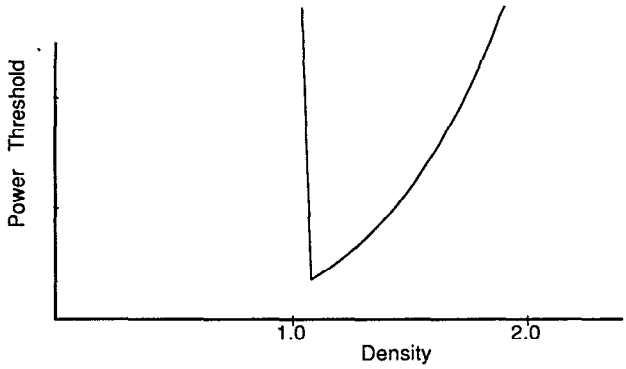

FIG. 6. Scaling of power threshold with density (arbitrary units).

The dependence of the power threshold, Q_c, on the magnetic field is as shown in Fig. 8. By comparison, the experimental power threshold increases with B, also, at constant plasma current.[7,10] There is no H-mode transition below a critical magnetic field because a maximum in the curve of heat flux versus temperature gradient does not occur for fields lower than the critical field. Such a critical magnetic field has not yet been seen experimentally.

The scaling with ion mass can also be obtained by using $\kappa_n \propto m_i^{1/2}$ and $\lambda_a \propto m_i$. Also, by assuming that $\kappa_{a0} \propto m_i^{-1/2}$ (consistent with the L-mode scaling[9] of energy confinement time $\tau_E \propto m_i^{1/2}$), the result shown in Fig. 9 is obtained.

The model predicts that the power threshold decreases with increasing ion mass, as seen in the experiments,[8] and also predicts that there would be a maximum ion mass for which the H mode could be obtained.

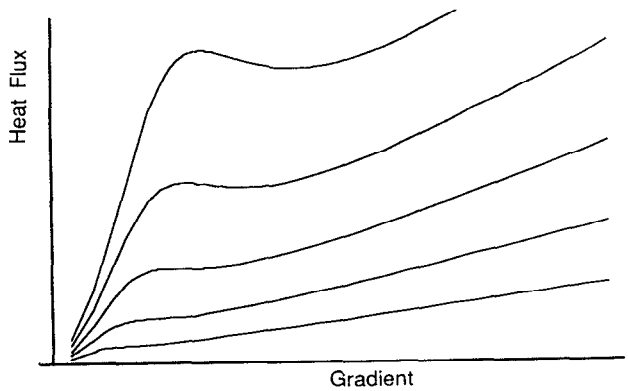

FIG. 7. Heat flux versus gradient for different densities. Density increases upward in this series of curves.

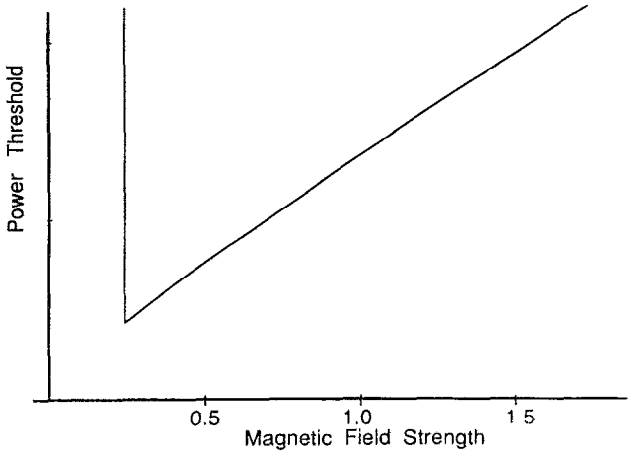

FIG. 8. Scaling of power threshold with magnetic field (arbitrary units).

The scaling laws obtained here numerically can also be derived in approximate form analytically, in the special case $\kappa_{a0}g \gg \kappa_n$, when the thermal conductivity in the L mode is much larger than in the H mode. (Since the relevant values are near the plasma edge, this is a realistic case.) Then, the equation for the heat flux can be approximated as follows:

$$\mathcal{Q}(g) \simeq \kappa_{a0} g^2/(1+\lambda_a g^4). \tag{33}$$

The maximum in this function occurs at $g_1 \simeq \lambda_a^{-1/4}$ and so the power threshold is

$$Q_c \equiv \mathcal{Q}(g_1) \simeq \kappa_{a0}/2\lambda_a^{1/2}. \tag{34}$$

Using the assumption of drift-wave turbulence, $\lambda_a^{1/2} \sim n^{-2}B^{-1}m_i^{-1/2}$, and the somewhat arbitrary choice $\kappa_{a0} \sim n^2 m_i^{-1/2}$, the scaling of the power threshold is

$$Q_c \sim n^4 B/m_i. \tag{35}$$

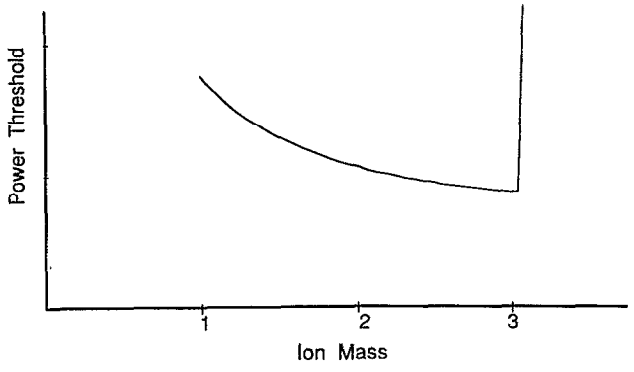

FIG. 9. Scaling of power threshold with ion mass (arbitrary units).

The linear dependence on magnetic field agrees with experiment, and the dependence on ion mass is about right, but the density dependence is too strong (Q_c should be linear in density).

IX. DISCUSSION

The picture of the L- to H-mode transition that is implied by this model is the following. After the auxiliary heating begins (or after the initiation of the discharge in the case of Ohmic heating), the heat flux at the plasma boundary gradually increases. The plasma near the edge goes through a sequence of quasisteady states, with the edge temperature gradient determined by the edge heat flux and the turbulent thermal transport. When the edge heat flux reaches a critical value (the power threshold for the H-mode transition), the edge temperature gradient increases rapidly, until a new quasiequilibrium is reached. In this new quasiequilibrium state, the large temperature gradient near the edge drives a large sheared poloidal flow, which causes a sheared radial electric field to appear (since the toroidal momentum input has not changed). The sheared $\mathbf{E}\times\mathbf{B}$ flow then suppresses the turbulent transport, allowing the edge temperature gradient to remain large. The temperature profile then appears to have a "pedestal," and the energy confinement time is significantly larger; the poloidal rotation has increased significantly, as seen in the experiments.

During the short time this transition is taking place, there would be a radial polarization current,[13] driven by the changing radial electric field, and this would create a toroidal torque that would change the toroidal rotation, according to Eq. (10). This current would be inward, since the radial electric field is becoming more negative, and would cause the toroidal corotation to slow briefly, as is, in fact, observed in the DIII-D experiments.[2]

Thus the simple model thermal conductivity predicts several features similar to those seen in the experimental results for the L- to H-mode transition. The following problems exist with the conclusions of the model, however.

(1) The energy confinement time is predicted to be neoclassical at large values of heating power, whereas experimentally it shows a degradation with power similar to that in the L mode. The neoclassical expression should therefore probably be replaced by a second turbulent contribution, which is not affected by poloidal rotation shear.

(2) The scaling of power threshold with plasma current I_p predicted by this model is wrong: since $\tau_E \propto I_p$ experimentally,[8,9] it follows that κ_{a0}, as well as κ_n, must depend upon current, and so will the power threshold Q_c. But Q_c is found experimentally to be independent of I_p at constant density and magnetic field. The coefficient of the velocity shear term must therefore also depend upon current, which implies a different model of turbulence than has been considered here.

It is also a shortcoming of the simple calculation presented here that the temperature dependence of the coefficients has been omitted. Also, all density gradient terms were ignored, and these are not small at the edge of the plasma. The effects of the latter are expected to contain the

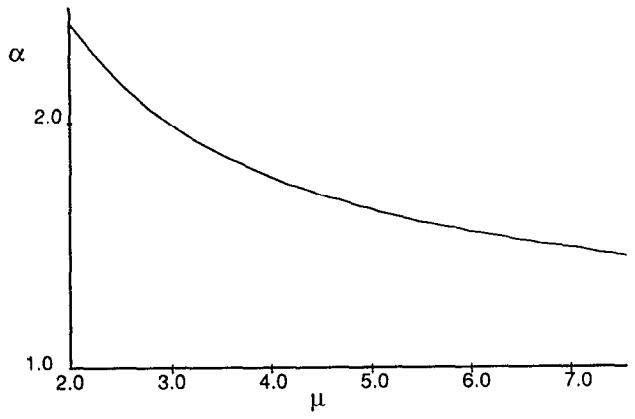

FIG. 10. Critical exponent for the bifurcation as a function of the parameter μ, defined in the text.

grad-B drift direction dependence of the power threshold,[14] since this has been shown to affect particle confinement near the edge.[15]

A question concerning the generality of the bifurcation phenomenon predicted by this model may be expressed as follows. Given a thermal conductivity in the form

$$\kappa=\kappa_n+\frac{\kappa_{a0}|\partial T/\partial r|}{1+\gamma_a|\partial u_\theta/\partial r|^\alpha}, \tag{36}$$

for what values of α is there a maximum in the local heat flux versus temperature gradient? For the neoclassical relationship between u_θ and $\partial T/\partial r$, the necessary values of the exponent α lie above the critical curve shown in Fig. 10, in which the important parameter is seen to be $\mu\equiv(\kappa_{a0}/\kappa_n\lambda_a^{(1/2\alpha)})$.

A related question concerns the density dependence assumed for the turbulent transport coefficient κ_{a0}. If it is assumed that $\kappa_{a0}\propto n^p$, how does the existence of a density threshold depend on the value of p that is used? With $\kappa_n\propto n^2$ and $\lambda_a\propto n^{-4}$, the coefficient μ defined previously becomes

$$\mu\propto n^{p-2+2/\alpha}. \tag{37}$$

Holding α fixed and varying the density, a critical density will correspond to crossing the curve in Fig. 10. For definiteness, let $\alpha=2$ so that the exponent of the density in the expression for μ is $p-1$. Then it is clear that, for the $p=1$, there is no dependence on density, so there will be no density threshold. Also, for $p>1$, increasing the density means increasing μ, so there will be a lower critical density: the density must exceed this threshold value in order that a bifurcation be possible. And finally, for $p<1$, increasing the density means decreasing μ, so there will be an upper critical density: the density must be less than this value for a bifurcation to be possible. The experimental results suggest that $p=2$, which was used in this paper, is an appropriate choice.

X. SUMMARY

A simple model for the thermal conductivity as a function of the temperature gradient, which was motivated by recent work on turbulence,[4] leads to a thermal confinement bifurcation with properties similar to the L- to H-mode transition seen experimentally in tokamaks. The poloidal rotation is assumed to be neoclassical, in contrast to the model of Shaing and Crume.[3] The following results are obtained.

(1) Temperature profiles in the H mode have an edge pedestal. Poloidal rotation and rotation shear are significantly larger in the H mode. The confinement time for an H-mode profile is significantly larger than for an L-mode profile with nearly the same heating power. The confinement time exhibits power hysteresis.

(2) A temperature-gradient-dependent model shows power degradation of confinement time in the L mode, although not in the H mode, and critical values of density and magnetic field, below which the H mode does not occur.

(3) The power threshold increases with increasing density and magnetic field, at constant plasma current, and decreases with increasing ion mass, as in the experiments.

ACKNOWLEDGMENTS

The author has benefited from discussions with H. Biglari, K. H. Burrell, P. H. Diamond, R. J. Groebner, Y. B. Kim, D. W. Ross, G. M. Staebler, and R. E. Waltz.

This is a report of work sponsored by the U.S. Department of Energy under Contract No. DE-AC03-89ER53277.

APPENDIX: NEOCLASSICAL POLOIDAL ROTATION

The poloidal flow is determined by the steady-state parallel momentum equation, Eq. (11), where the parallel viscous stress is given by

$$\langle\mathbf{B}\cdot(\nabla\cdot\mathbf{\Pi}_i)\rangle=-\left\langle(\hat{b}\cdot\nabla B)m_i\int d^3v(v_\parallel^2-v_\perp^2/2)f_i\right\rangle, \tag{A1}$$

with f_i the ion distribution function. This function is a solution of the drift kinetic equation. By generalizing the work in Ref. 16, assuming that the flow is of order $(\rho_i/L_\perp)v_{thi}$ this equation is found to be

$$\begin{aligned}
&v_\parallel\hat{b}\cdot\nabla f_i-\frac{v_\perp^2}{2B}(\hat{b}\cdot\nabla B)\left(\frac{\partial f_i}{\partial v_\parallel}-\frac{v_\parallel}{v_\perp}\frac{\partial f_i}{\partial v_\perp}\right)-C_{ii}^{l}f_i\\
&\quad=-\frac{\mathbf{v}_D\cdot\nabla T}{T}\left(\frac{v^2}{v_{thi}^2}-\frac{5}{2}\right)F_i+v_\parallel\hat{b}\cdot(\nabla\mathbf{u}_i)\cdot\hat{b}\,\frac{\partial F_i}{\partial v_\parallel}\\
&\qquad+\frac{v_\perp}{2}[\nabla\cdot\mathbf{u}_i-\hat{b}\cdot(\nabla\mathbf{u}_i)\cdot\hat{b}\,]\frac{\partial F_i}{\partial v_\perp}\\
&\quad=-\frac{\mathbf{v}_D\cdot\nabla T}{T}\left(\frac{v^2}{v_{thi}^2}-\frac{5}{2}\right)F_i-\frac{m_i}{T_i}\left(v_\parallel^2-\frac{v_\perp^2}{2}\right)K_i(\hat{b}\cdot\nabla B)F_i,
\end{aligned} \tag{A2}$$

where $K_i=u_{i\theta}/B_\theta$. The guiding center drift velocity is

$$\mathbf{v}_D=(c/B)\,\hat{b}\times\nabla\Phi+(\hat{b}/\Omega_i)\times(\mu\nabla B+v_\parallel^2\hat{b}\cdot\nabla\hat{b}), \tag{A3}$$

with $\hat{b}=\mathbf{B}/B$.

The drift kinetic equation can be written in the form

$$(\mathscr{T}_i-C_{ii})f_i=-\mathscr{R}, \tag{A4}$$

where $\mathscr{R}$ is the right-hand side, which consists of two terms, proportional to the poloidal flow and the temperature gradient. The solution for large collisionality, $\nu_{*i}\gg 1$, where

$$\nu_{*i}\equiv qR/(v_{\mathrm{th}i}\tau_{ii}\epsilon^{3/2}), \tag{A5}$$

with ϵ the inverse aspect ratio, can be written as

$$\begin{aligned} f_i&=C_{ii}^{-1}(\mathscr{I}-\mathscr{T}_iC_{ii}^{-1})^{-1}\mathscr{R}\\ &=C_{ii}^{-1}[\mathscr{I}+\mathscr{T}_iC_{ii}^{-1}+(\mathscr{T}_iC_{ii}^{-1})^2+\cdots]\mathscr{R}. \end{aligned} \tag{A6}$$

It follows that the parallel viscous stress has the form

$$\begin{aligned} \frac{1}{B_\theta}\langle\mathbf{B}\cdot(\nabla\cdot\mathbf{\Pi}_i)\rangle=&\left(\frac{c_1}{\nu_{*i}}+\frac{c_3}{\nu_{*i}^3}+\cdots\right)\frac{\partial T_i}{\partial r}+\left(\frac{d_1}{\nu_{*i}}\right.\\ &\left.+\frac{d_3}{\nu_{*i}^3}+\cdots\right)u_{i\theta}, \end{aligned} \tag{A7}$$

with only odd powers of collisionality appearing because only the $l=2$ Legendre polynomial component of f_i contributes to the stress. Setting this stress equal to zero, the poloidal flow is given by

$$u_\theta=-\left(\frac{d_1}{\nu_{*i}}+\frac{d_3}{\nu_{*i}}+\cdots\right)^{-1}\left(\frac{c_1}{\nu_{*i}^3}+\frac{c_3}{\nu_{*i}^3}+\cdots\right)\frac{\partial T_i}{\partial r}. \tag{A8}$$

The coefficients d_1 and c_1 in this expression are known, but the others are not. The result can be written as

$$u_\theta=-\frac{c}{eB}\mu(\nu_{*i})\frac{\partial T}{\partial r}, \tag{A9}$$

where the proportionality coefficient has the approximate form

$$\mu(\nu_{*i})\simeq\mu_0+\frac{\mu_1}{(\nu_{*i})^2}, \tag{A10}$$

for $\nu_{*i}\gg 1$, where $\mu_0=1.7$ (the Pfirsch–Schlüter limit). It is reasonable to assume that $\mu_1<0$ in order to facilitate the transition to the low collisionality limit, where $\mu(\nu_{*i})$ has the opposite sign.

Equation (A2) implies that the poloidal rotation direction is reversed when the direction of the toroidal magnetic field is reversed, because the drift velocity term $\mathbf{v}_D\cdot\nabla T$ changes sign, but the other terms on the right-hand side do not.

[1] F. Wagner, G. Becker, K. Behringer, D. Campbell, A. Eberhagen, W. Englehardt, G. Fussmann, O. Gehre, J. Gernhardt, G. v. Gierke, G. Haas, M. Huang, F. Karger, M. Keilhacker, O. Klüber, M. Kornherr, K. Lackner, G. Lisitano, G. G. Lister, H. M. Mayer, D. Meisel, E. R. Müller, H. Murmann, H. Niedermeyer, W. Poschenrieder, H. Rapp, H. Röhr, F. Schneider, G. Siller, E. Speth, A. Stäbler, K. H. Steuer, G. Venus, O. Vollmer, and Z. Yü, Phys. Rev. Lett. **49**, 1408 (1982).

[2] R. J. Groebner, K. H. Burrell, and R. P. Seraydarian, Phys. Rev. Lett. **64**, 3015 (1990).

[3] K. C. Shaing and E. C. Crume, Jr., Phys. Rev. Lett. **63**, 2369 (1989).

[4] H. Biglari, P. H. Diamond, and P. W. Terry, Phys. Fluids B **2**, 1 (1990).

[5] F. L. Hinton and R. D. Hazeltine, Rev. Mod. Phys. **48**, 239 (1976); S. P. Hirshman and D. J. Sigmar, Nucl. Fusion **21**, 1079 (1981).

[6] A. B. Hassam and R. M. Kulsrud, Phys. Fluids **21**, 2271 (1978).

[7] T. N. Carlstrom, M. Shimada, K. H. Burrell, J. C. DeBoo, P. Gohil, R. J. Groebner, C. Hsieh, M. Matsumoto, and P. Trust, in *Proceedings of the 16th European Conference on Controlled Fusion and Plasma Physics*, Venice (EPS, Geneva, 1989), Vol. I, p. 241.

[8] K. H. Burrell, S. L. Allen, G. Bramson, N. H. Brooks, R. W. Callis, T. N. Carlstrom, M. S. Chu, A. P. Colleraine, D. Content, J. C. DeBoo, R. R. Dominguez, J. R. Ferron, R. L. Freeman, P. Gohil, C. M. Greenfield, R. J. Groebner, G. Haas, W. W. Heidbrink, D. N. Hill, F. L. Hinton, R.-M. Hong, W. Howl, C. L. Hseih, G. L. Jackson, G. L. Jahns, R. A. James, A. G. Kellman, J. Kim, L. L. Lao, E. A. Lazarus, T. Lehecka, J. Lister, J. Lohr, T. C. Luce, J. L. Luxon, M. A. Mahdavi, H. Matsumoto, M. Mayberry, C. P. Moeller, Y. Nayatani, T. Ohkawa, N. Ohyabu, T. Okazaki, T. H. Osborne, D. O. Overskei, T. Ozeki, A. Peebles, S. Perkins, M. Merry, P. I. Petersen, T. W. Petrie, R. Philipona, J. C. Phillips, R. Pinsker, P. A. Politzer, G. D. Porter, R. Prater, M. E. Rensink, M. J. Schaffer, D. P. Schissel, J. T. Scoville, R. P. Seraydarian, M. Shimada, T. C. Simonen, R. T. Snider, G. M. Staebler, B. W. Stallard, R. D. Stambaugh, R. D. Stav, H. St. John, R. E. Stockdale, E. J. Strait, P. L. Taylor, T. S. Taylor, P. K. Trost, U. Stroth, R. E. Waltz, S. M. Wolfe, R. D. Wood, and D. Wroblewski, Plasma Phys. Controlled Fusion **31**, 1649 (1989).

[9] S. M. Kaye and R. J. Goldston, Nucl. Fusion **25**, 65 (1985).

[10] R. J. Goldston (private communication).

[11] R. E. Waltz, Phys. Fluids **29**, 3684 (1986).

[12] J. W. Connor and J. B. Taylor, Phys. Fluids **27**, 2676 (1984).

[13] F. L. Hinton and J. A. Robertson, Phys. Fluids **27**, 1243 (1984); S. P. Hirshman, Nucl. Fusion **18**, 917 (1978).

[14] F. Wagner, R. Bartiromo, G. Becker, H. S. Bosch, A. Eberhagen, G. Fussmann, O. Gehre, J. Gernhardt, G. v. Gierke, E. Glock, O. Gruber, G. Haas, G. Janeschitz, F. Karger, M. Keilhacker, A. Kislyakov, O. Klüber, M. Kornherr, P. B. Kotzé, K. Lackner, M. Lenoci, G. Lisitano, A. Mahdavi, H.-M. Mayer, K. McCormick, D. Meisel, V. Mertens, E. R. Müller, H. Murmann, H. Niedermeyer, W. Poschenrieder, H. Rapp, F. Ryter, J. Roth, F. Schneider, G. Siller, P. Smeulders, F. Söldner, E. Speth, K. Steinmetz, K.-H. Steuer, and O. Vollmer, Nucl. Fusion **25**, 1490 (1985).

[15] F. L. Hinton and G. M. Staebler, Nucl. Fusion **29**, 405 (1989).

[16] F. L. Hinton and S. K. Wong, Phys. Fluids **28**, 3082 (1985).